Article

Cobalt(III) Corroles as Electrocatalysts for the Reduction of Dioxygen: Reactivity of a Monocorrole, Biscorroles, and Porphyrin–Corrole Dyads

Karl M. Kadish, Laurent Frmond, Zhongping Ou, Jianguo Shao, Chunnian Shi, Fred C. Anson, Fabien Burdet, Claude P. Gros, Jean-Michel Barbe, and Roger Guilard

J. Am. Chem. Soc., **2005**, 127 (15), 5625-5631• DOI: 10.1021/ja0501060 • Publication Date (Web): 26 March 2005

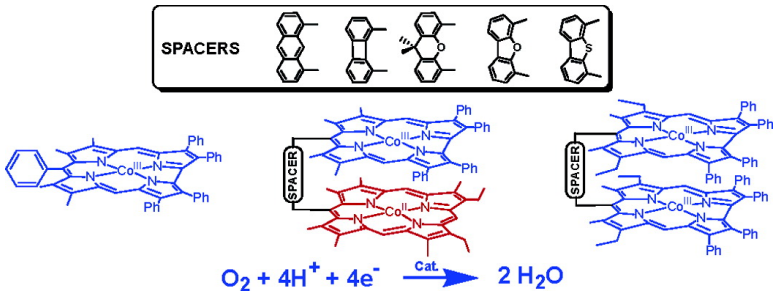

More About This Article

Additional resources and features associated with this article are available within the HTML version:

- Supporting Information
- Links to the 10 articles that cite this article, as of the time of this article download
- Access to high resolution figures
- Links to articles and content related to this article
- Copyright permission to reproduce figures and/or text from this article

View the Full Text HTML

J|A|C|S
ARTICLES
Published on Web 03/26/2005

Cobalt(III) Corroles as Electrocatalysts for the Reduction of Dioxygen: Reactivity of a Monocorrole, Biscorroles, and Porphyrin−Corrole Dyads

Karl M. Kadish,*,† Laurent Frémond,† Zhongping Ou,† Jianguo Shao,† Chunnian Shi,‡ Fred C. Anson,‡ Fabien Burdet,§ Claude P. Gros,§ Jean-Michel Barbe,§ and Roger Guilard*,§

Contribution from the Department of Chemistry, University of Houston, Houston, Texas 77204-5003, Division of Chemistry and Chemical Engineering, Arthur Amos Noyes Laboratory, California Institute of Technology, Pasadena, California 91125, and Université de Bourgogne, LIMSAG (UMR 5633), 6 boulevard Gabriel, 21100 Dijon, France

Received January 7, 2005; E-mail: kkadish@uh.edu; rguilard@u-bourgogne.fr

Abstract: Three series of cobalt(III) corroles were tested as catalysts for the electroreduction of dioxygen to water. One was a simple monocorrole represented as $(Me_4Ph_5Cor)Co$, one a face-to-face biscorrole linked by an anthracene (A), biphenylene (B), 9,9-dimethylxanthene (X), dibenzofuran (O) or dibenzothiophene (S) bridge, $(BCY)Co_2$ (with Y = A, B, X, O or S), and one a face-to-face bismacrocyclic complex, $(PCY)Co_2$, containing a Co(II) porphyrin and a Co(III) corrole also linked by one of the above rigid spacers (Y = A, B, X, or O). Cyclic voltammetry and rotating ring−disk electrode voltammetry were both used to examine the catalytic activity of the cobalt complexes in acid media. The mixed valent Co(II)/Co(III) complexes, $(PCY)Co_2$, and the biscorrole complexes, $(BCY)Co_2$, which contain two Co(III) ions in their air-stable forms, all provide a direct four-electron pathway for the reduction of O_2 to H_2O in aqueous acidic electrolyte when adsorbed on a graphite electrode, with the most efficient process being observed in the case of the complexes having an anthracene spacer. A relatively small amount of hydrogen peroxide was detected at the ring electrode in the vicinity of $E_{1/2}$ which was located at 0.47 V vs SCE for $(PCA)Co_2$ and 0.39 V vs SCE for $(BCA)Co_2$. The cobalt(III) monocorrole $(Me_4Ph_5Cor)Co$ also catalyzes the electroreduction of dioxygen at $E_{1/2} = 0.38$ V with the final products being an approximate 50% mixture of H_2O_2 and H_2O.

Introduction

Several porphyrin−corrole,[1] biscorrole,[1] and bisporphyrin[2−8] dyads linked in a cofacial configuration have been synthesized and examined as to their electrochemical reactivity with small molecules such as O_2 or CO. One such compound is the anthracenyl-bridged porphyrin−corrole dyad $(PCA)Co_2$, **1a**, (Chart 1) which strongly binds O_2 in air giving a stable bis-Co(III) μ-superoxo complex as evidenced by its 15-line ESR spectrum.[9] A similar dicobalt face-to-face anthracenyl-bridged bisporphyrin[2,10] is able to catalyze the four-electron electroreduction of O_2 in acidic media, and it was of interest to examine catalytic properties of the related mixed oxidation state porphyrin−corrole dyads **1a**−**1d** and the Co(III) biscorrole dyads **3a**−**3e** (Chart 1) under similar experimental conditions.

Metallocorroles have been examined as to their catalytic properties in oxidation reactions[11,12] and their affinity for dioxygen,[13] but nothing has been reported as to their ability to catalyze the electroreduction of O_2 when adsorbed on an electrode surface. The main difference between the cobalt corroles and previously studied cobalt porphyrins is the oxidation state of the central metal ion. The uncharged cobalt mono- and bisporphyrins contain Co(II) ions, while the neutral porphyrin−corrole dyads, **1a**−**1d**, contain a Co(III) corrole linked to a Co(II) porphyrin. In contrast, the biscorrole dyads $(BCY)Co_2$, **3a**−**3e**, and the uncharged monocorrole **2** contain only Co(III) ions.

One goal of the present study was to examine the redox properties of the three series of corroles in acidic media and

† University of Houston.
‡ California Institute of Technology.
§ Université de Bourgogne.

(1) Guilard, R.; Barbe, J.-M.; Stern, C.; Kadish, K. M. In *The Porphyrin Handbook*; Kadish, K. M., Smith, J. R. L., Guilard, R., Eds.; Academic Press: Boston, 2003; Vol. 18, pp 303−349.
(2) Collman, J. P.; Boulatov, R.; Sunderland, C. J. *The Porphyrin Handbook*; Academic Press: Boston, 2003; Vol. 11, pp 1−49.
(3) Le Mest, Y.; L'Her, M.; Hendricks, N. H.; Kim, K.; Collman, J. P. *Inorg. Chem.* **1992**, *31*, 835−847.
(4) Le Mest, Y.; L'Her, M. *J. Chem. Soc., Chem. Commun.* **1995**, 1441−1442.
(5) Le Mest, Y.; L'Her, M.; Saillard, J.-Y. *Inorg. Chim. Acta* **1996**, *248*, 181−191.
(6) Le Mest, Y.; Inisan, C.; Laouenan, A.; L'Her, M.; Talarmin, J.; El Khalifa, M.; Saillard, J.-Y. *J. Am. Chem. Soc.* **1997**, *119*, 6095−6106.
(7) Chang, C. J.; Loh, Z.-H.; Shi, C.; Anson, F. C.; Nocera, D. G. *J. Am. Chem. Soc.* **2004**, *126*, 10013−10020.
(8) Collman, J. P.; Wagenknecht, P. S.; Hutchison, J. E. *Angew. Chem., Int. Ed. Engl.* **1994**, *33*, 1537−1554.
(9) Guilard, R.; Jérome, F.; Gros, C. P.; Barbe, J.-M.; Ou, Z.; Shao, J.; Kadish, K. M. *C. R. Acad. Sci., Ser. IIc: Chim.* **2001**, *4*, 245−254.
(10) Chang, C. K.; Liu, H.-Y.; Abdalmuhdi, I. *J. Am. Chem. Soc.* **1984**, *106*, 2725−2726.
(11) Collman, J. P.; Zeng, L.; Decreau, R. A. *Chem. Commun.* **2003**, *24*, 2974−2975.
(12) Mahammed, A.; Gray, H. B.; Meier-Callahan, A. E.; Gross, Z. *J. Am. Chem. Soc.* **2003**, *125*, 1162−1163.
(13) Ramdhanie, B.; Telser, J.; Caneschi, A.; Zakharov, L. N.; Rheingold, A. L.; Goldberg, D. P. *J. Am. Chem. Soc.* **2004**, *126*, 2515−2525.

Chart 1

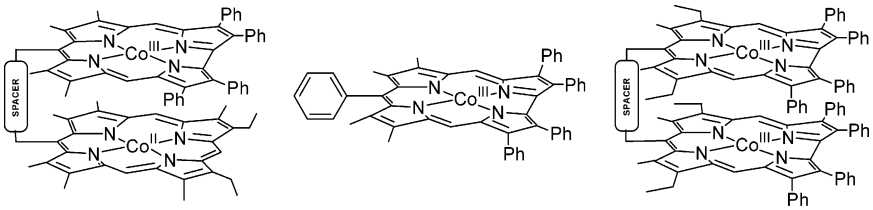

(PCY)Co_2, 1 (Me$_4$Ph$_5$Cor)Co, 2 (BCY)Co_2, 3

SPACERS (Y)

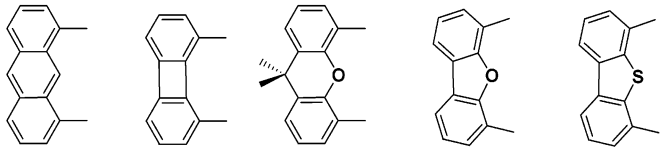

(PCA)Co_2: 1a (PCB)Co_2: 1b (PCX)Co_2: 1c (PCO)Co_2: 1d

(BCA)Co_2: 3a (BCB)Co_2: 3b (BCX)Co_2: 3c (BCO)Co_2: 3d (BCS)Co_2: 3e

another was to examine their use as catalysts for the reduction of O_2 at a graphite electrode. All 10 corroles examined in this study are well characterized as to their electrochemistry under N_2 in a variety of nonaqueous solvents.[9,14−17] (Me$_4$Ph$_5$Cor)-Co^{III}, **2**, can be reversibly reduced to its Co(II) form at $E_{1/2}$ = −0.15 to −0.17 V vs SCE in CH_2Cl_2, PhCN, or THF.[14] Slightly more negative potentials are observed for the Co(III)/Co(II) process of the biscorroles (BCY)Co_2[15,16] and porphyrin−corroles (PCY)Co_2[15] under similar experimental conditions.

Of more relevance to the present work are the potentials where the three investigated corroles are oxidized to their higher, formally Co(IV) and Co(IV) π-cation radical oxidation states. These electrode reactions occur at $E_{1/2}$ = 0.47 and 0.82 V for (Me$_4$Ph$_5$Cor)Co^{III}, **2**, in PhCN 0.1 M TBAP and at $E_{1/2}$ = 0.53 and 0.73 V in THF giving [**2**]$^+$ and [**2**]$^{2+}$ in both solvents.[14] A splitting of the first redox process of **2** is observed in CH_2Cl_2 due to the presence of dimers.[14] As will be described, both series of biscobalt complexes **1** and **3** can serve as catalysts for the four-electron electroreduction of dioxygen in an air-saturated aqueous acidic solution containing 1 M $HClO_4$. The onset potentials of the catalytic reduction for both biscobalt complexes are comparable to the potentials for the formal Co(IV)/Co(III) processes of the catalysts in nonaqueous media. This result is consistent with the binding of O_2 by the Co(III) form of the compounds and is also consistent with the previously described μ-superoxo species that are formed in the reaction between O_2 and (PCA)Co_2.[9]

Experimental Section

Chemicals and Corroles. Unless otherwise noted, all chemicals were obtained commercially and used without further purification. High-purity N_2 gas was purchased from Matheson-Trigas. Organic solvents and mineral acids were of reagent grade and were used as supplied except for benzonitrile (PhCN) which was purified by passage through a column of activated Linde 3 Å molecular sieves followed by distillation under reduced pressure. All subsequent aqueous solutions were prepared with deionized water of resistivity not less than 18 MΩ cm. The synthesis and characterization of the cobalt complexes used in this study [(PCY)Co_2, (BCY)Co_2, and (Me$_4$Ph$_5$Cor)Co] were reported elsewhere.[15,18] Thin layers of PhCN separating the polished edge-plane pyrolytic graphite electrode from aqueous acidic solutions were prepared and utilized according to procedures described in the literature.[19]

Electrochemical Apparatus and Procedures. All electrochemical data were collected using a three-electrode cell. The three-electrode system consisted of a platinum ring−graphite disk working electrode, a platinum wire as the auxiliary electrode, and a commercial saturated calomel electrode (SCE) as the reference which was separated from the bulk of the solution by means of a salt bridge. The KCl solution in the SCE was changed periodically to maintain the correct potential that was checked using a standard solution for redox potential measurements.[20] An aqueous Ag/AgCl/3 M NaCl reference electrode (−40 mV vs SCE) was employed for thin-layer experiments.

All electrochemical experiments were conducted at ambient laboratory temperature (22 ± 2 °C). Cyclic voltammetry and rotating disk experiments were carried out using a Pine Instrument model AFMSR rotator linked to an EG&G Princeton Applied Research (PAR) model 263A potentiostat/galvanostat. The potentiostat was monitored by an IBM-compatible PC microcomputer controlled by the software M270 (EG&G PARC). A RDE4 bipotentiostat (Pine Instrument) was employed with a HP 7090A three-channel digital plotter for rotating ring−disk electrochemical experiments. The rotating ring−disk electrode (RRDE), purchased from the Pine Instrument Co., consisted of a platinum ring and a removable graphite disk.

The equations used to calculate the average number of electrons transferred n and the percentage of H_2O_2 formed at the electrode are $n = 4I_D/(I_D + I_R/N)$ and % $H_2O_2 = 100(2I_R/N)/(I_D + I_R/N)$, respectively, where I_D is the faradic current at the disk and I_R is the faradic current at the ring.[21] The intrinsic value of the collection efficiency was determined to be N = 0.24 using the $Fe(CN)_6^{3-/4-}$ redox couple in 1 M KCl. Just before it was coated with the catalyst, the edge-plane pyrolytic graphite disk (A = 0.282 cm^2) was polished to a rough finish

(14) Kadish, K. M.; Shao, J.; Ou, Z.; Gros, C. P.; Bolze, F.; Barbe, J.-M.; Guilard, R. *Inorg. Chem.* **2003**, *42*, 4062−4070.
(15) Kadish, K. M.; Ou, Z.; Shao, J.; Gros, C. P.; Barbe, J.-M.; Jérome, F.; Bolze, F.; Burdet, F.; Guilard, R. *Inorg. Chem.* **2002**, *41*, 3990−4005.
(16) Guilard, R.; Jérome, F.; Barbe, J.-M.; Gros, C. P.; Ou, Z.; Shao, J.; Fischer, J.; Weiss, R.; Kadish, K. M. *Inorg. Chem.* **2001**, *40*, 4856−4865.
(17) Guilard, R.; Gros, C. P.; Bolze, F.; Jérome, F.; Ou, Z.; Shao, J.; Fischer, J.; Weiss, R.; Kadish, K. M. *Inorg. Chem.* **2001**, *40*, 4845−4855.
(18) Barbe, J.-M.; Burdet, F.; Espinosa, E.; Gros, C. P.; Guilard, R. *J. Porphyrins Phthalocyanines* **2003**, *7*, 365−374.
(19) Shi, C.; Anson, F. C. *Anal. Chem.* **1998**, *70*, 3114−3118.
(20) Light, T. S. *Anal. Chem.* **1972**, *44*, 1038−1039.
(21) Lefevre, M.; Dodelet, J.-P. *Electrochim. Acta* **2003**, *48*, 2749−2760.

with 600 grit SiC paper, rinsed with water, and wiped off to remove any free graphite particles. The molecular catalyst was irreversibly adsorbed on the electrode surface by means of a dip-coating procedure; the freshly polished electrode was dipped for 5 s in a 0.1 mM solution of the catalyst in $CHCl_3$, transferred rapidly to pure $CHCl_3$ for 1−2 s, and then dried.[22] After coating, the ring−disk electrode was introduced into air-saturated aqueous acid 1 M $HClO_4$. Particular care was exercised to ensure high reactivity of the Pt ring toward H_2O_2. Immediately prior to use, Pt was cleaned with a 5-μm alumina slurry (Buehler MICROPOLISH II polishing suspension) on a polishing cloth (Buehler MICROCLOTH), rinsed successively with water and methanol, dried, and activated by cycling between 1.20 and −0.24 V in 1 M $HClO_4$ until reproducible voltammograms were obtained.[23,24] During polishing of the Pt ring, the graphite disk was removed to avoid contamination of the Pt with graphite particles and to preserve the integrity of the graphite surface.

For $(Me_4Ph_5Cor)Co$- and $(PCA)Co_2$-catalyzed dioxygen reduction, the slopes of the Koutecký−Levich plots were determined by linear regression analysis of data acquired at 100, 400, 900, 1600, 2500, and 3600 rpm (rpm = revolutions per minute). The diffusion-limiting currents for the reduction of O_2 in aqueous solution at the rotating disk electrode were calculated using the following parameters: kinematic viscosity of H_2O at 25 °C, 0.01 $cm^2\ s^{-1}$; solubility of O_2 in air-saturated 1 M $HClO_4$, 0.24 mM; diffusion coefficient of O_2, 1.7×10^{-5} $cm^2\ s^{-1}$.[22] The solubility of dioxygen in 1 M $HClO_4$ was calculated by using the Setschenow equation ($\ln\{m_{O_2}^0/m_{O_2}\} = k_s \times m$) and the Pitzer equation[25] ($k_s(HClO_4) = 2\lambda_{O_2,H^+} + 2\lambda_{O_2,ClO_4^-}$) where m is the molality (mol kg^{-1}) of $HClO_4$, $m_{O_2}^0$ is the molality of O_2 in pure water,[26] $\lambda_{O_2,H^+} = 0.0353$, and $\lambda_{O_2,ClO_4^-} = -0.007$.[27]

Results and Discussion

Redox Properties of Complexes 1a, 2, and 3a and Catalytic Reduction of O_2. A detailed discussion is given for compounds **1a**, **2**, and **3a**, and this is followed by data on the other linked derivatives in the two series of biscobalt complexes.

The three series of cobalt complexes were applied to an edge-plane pyrolytic graphite (EPG) electrode by irreversible adsorption from a dilute chloroform solution. Cyclic voltammograms recorded at a graphite disk coated with complex **1a** are illustrated in Figure 1A. In the absence of dioxygen, the response of the modified graphite electrode is characterized by a redox process centered at $E_{1/2} = 0.38$ V in 1 M $HClO_4$ ($E_{pc} = 0.36$ V, $E_{pa} = 0.40$ V). When the solution is saturated with air, a larger cathodic peak is observed at almost the same potential of $E_p = 0.40$ V. The reduction of O_2 at an uncoated graphite electrode occurs at $E_p = -0.34$ V which indicates that complex **1a** catalyzes the electroreduction of dioxygen when adsorbed on graphite.

A catalytic reduction wave of dioxygen is also observed at a rotating platinum ring−graphite disk electrode modified by adsorption of complex **1a** on the disk as illustrated in Figure 1B. This RRDE voltammogram was obtained by scanning the disk potential from 0.70 to 0.00 V vs SCE at a rotation speed of 100 rpm while holding the ring potential at 1.10 V so that any H_2O_2 formed at the disk could be detected at the ring. Under these conditions, the anodic ring current results from the oxidation of H_2O_2 to O_2. As seen in the figure, the disk current begins to increase at about 0.60 V, and the plateau is reached at 0.30 V. At about 0.26 V, the current begins to decrease slightly and then rises again as the potential is scanned to more negative values. A similar behavior was previously observed for $(FTF4)Co_2$[28,29] (FTF4 = face-to-face porphyrin dimer with a linking group of 4 atoms) and biscobalt "Pacman" type bisporphyrins.[10,30,31] Only a relatively small amount of hydrogen peroxide is detected at the ring electrode in the vicinity of $E_{1/2}$ when the reaction is carried out in air-saturated $HClO_4$ (Table 1). The value of the disk current at $E_{1/2}$ corresponds to an apparent number of electrons transferred of $n = 3.9$. From the data in the figure, we cannot say which of the two cobalt centers is reduced first in $(PCA)Co_2$ (that of the corrole or that of the porphyrin), but there is no doubt that the redox process at $E_{1/2} = 0.38$ V in $HClO_4$ under argon corresponds to the electroreduction of O_2 to give H_2O at $E_p = 0.40$ V under air.

The electrochemical and electrocatalytic properties of the monocorrole **2** in $HClO_4$ differ from that of the dicobalt porphyrin−corrole **1a** under the same solution conditions. The

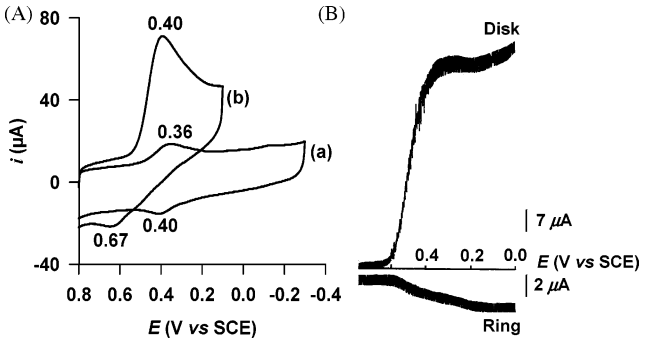

Figure 1. (A) Cyclic voltammograms of **1a** adsorbed on an EPG electrode. Supporting electrolyte: 1 M $HClO_4$ (a) saturated with argon and (b) saturated with air. Scan rate: 50 mV s^{-1}. (B) Reduction of O_2 at a rotating ring (Pt)−disk (EPG) electrode in air-saturated 1 M $HClO_4$. The potential of the ring electrode was maintained at 1.1 V. Rotation rate: 100 rpm. Scan rate: 5 mV s^{-1}.

Table 1. Electroreduction of Dioxygen by Adsorbed Dicobalt Porphyrin−Corroles and Biscorroles in Air-Saturated 1 M $HClO_4$

cmpd		E_p[a]	$E_{1/2}$[b]	n[c]
1a	$(PCA)Co_2$	0.40	0.47	3.9
1b	$(PCB)Co_2$	0.38	0.46	3.7
1c	$(PCX)Co_2$	0.38	0.45	3.7
1d	$(PCO)Co_2$	0.34	0.41	3.5
2	$(Me_4Ph_5Cor)Co$	0.36	0.38	2.9
3a	$(BCA)Co_2$	0.36	0.39	3.4
3b	$(BCB)Co_2$	0.35	0.37	2.4
3c	$(BCX)Co_2$	0.34	0.37	2.9
3d	$(BCO)Co_2$	0.33	0.35	3.4
3e	$(BCS)Co_2$	0.33	0.35	3.1

[a] Peak potential of the dioxygen reduction wave (V vs SCE). [b] Half-wave potential (V vs SCE) for dioxygen reduction at rotating disk electrode ($\omega = 100$ rpm). [c] The apparent number of electrons transferred per dioxygen molecule (n) at $E_{1/2}$ is calculated from $n = 4I_D/(I_D+I_R/N)$ where I_D and I_R are disk and ring currents, respectively, and N (= 0.24) is the collection efficiency of the ring−disk electrode.[21]

(22) Shi, C.; Anson, F. C. *Inorg. Chem.* **1998**, *37*, 1037−1043.
(23) Conway, B. E.; Angerstein-Kozlowska, H.; Sharp, W. B. A.; Criddle, E. E. *Anal. Chem.* **1973**, *45*, 1331−1336.
(24) Hsueh, K.-L.; Gonzalez, E. R.; Srinivasan, S. *Electrochim. Acta* **1983**, *28*, 691−697.
(25) Millero, F. J.; Huang, F. *J. Chem. Eng. Data* **2003**, *48*, 1050−1054.
(26) Millero, F. J.; Huang, F.; Laferiere, A. L. *Geochim. Cosmochim. Acta* **2002**, *66*, 2349−2359.
(27) Clegg, S. L.; Brimblecombe, P. *Geochim. Cosmochim. Acta* **1990**, *54*, 3315−3328.
(28) Collman, J. P.; Marrocco, M.; Denisevich, P.; Koval, C.; Anson, F. C. *J. Electroanal. Chem.* **1979**, *101*, 117−122.
(29) Collman, J. P.; Denisevich, P.; Konai, Y.; Marrocco, M.; Koval, C.; Anson, F. C. *J. Am. Chem. Soc.* **1980**, *102*, 6027−6036.
(30) Liu, H.-Y.; Abdalmuhdi, I.; Chang, C. K.; Anson, F. C. *J. Phys. Chem.* **1985**, *89*, 665−670.
(31) Chang, C. J.; Deng, Y.; Shi, C.; Chang, C. K.; Anson, F. C.; Nocera, D. G. *Chem. Commun.* **2000**, 1355−1356.

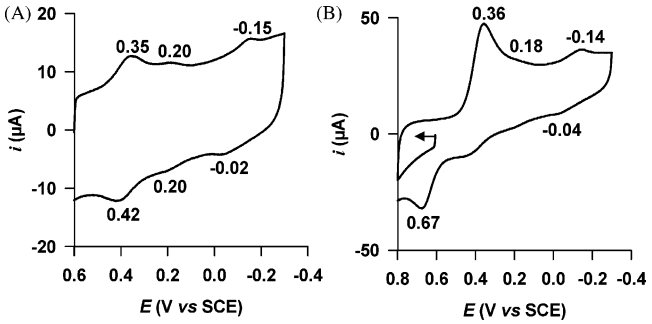

Figure 2. Cyclic voltammograms of **2** adsorbed on EPG electrode. Supporting electrolyte: 1 M $HClO_4$ saturated (A) with argon, (B) with air. Scan rate: 50 mV s^{-1}.

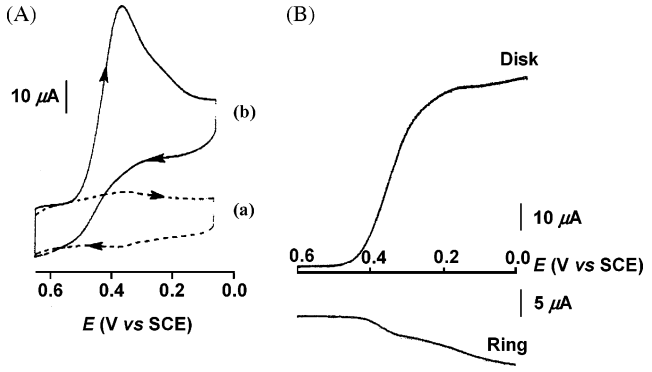

Figure 3. (A) Cyclic voltammograms of **3a** adsorbed on an EPG electrode. Supporting electrolyte: 1 M $HClO_4$ (a) saturated with argon and (b) saturated with air. Scan rate: 50 mV s^{-1}. (B) Reduction of O_2 at a rotating ring (Pt)−disk (EPG) electrode in air-saturated 1 M $HClO_4$. The potential of the ring electrode was maintained at 1.1 V. Rotation rate: 100 rpm. Scan rate: 5 mV s^{-1}.

cyclic voltammogram of **2** adsorbed on a graphite disk in the absence of dioxygen shows three reversible processes located at $E_{1/2}$ = 0.38, 0.20, and −0.08 V (Figure 2A). The three reactions can be related to similar reactions for the same compound in CH_2Cl_2 which occur at $E_{1/2}$ = 0.62, 0.45, and −0.15 V.[14,17] The electrochemical response at −0.15 V was assigned to the Co(III)/Co(II) couple.[17] In comparison with the same process of a structurally related porphyrin, (OEP)Co[32] ($E_{1/2}$ = 0.41 V) where OEP = octaethylporphyrin, the smaller ring size of the macrocyclic cavity[33] of **2** shifts the formal potential of the Co(III)/Co(II) couple by 490 mV to lower values in accordance with the fact that a corrole macrocycle stabilizes the Co(III) oxidation state whereas porphyrins stabilize cobalt in a +2 oxidation state.[1,33,34] The two processes at $E_{1/2}$ = 0.38 and 0.20 V for complex **2** suggest reduction via a dimeric species as is also observed in a nonaqueous solvent such as CH_2Cl_2.[14,17] The first reduction peak at E_p = 0.35 V in Figure 2A thus probably corresponds to formation of a monooxidized dimer, $[(\mathbf{2})_2]^+$, which is catalytically active toward the reduction of dioxygen as seen in Figure 2B by the substantially enhanced peak currents at E_p = 0.36 V in the presence of O_2.

Shown in Figure 3 are the cyclic voltammograms and rotating ring−disk electrode voltammograms responses obtained for $(BCA)Co_2$, **3a**, adsorbed on an EPG electrode in 1 M $HClO_4$. Results for the biscorrole **3a** parallel what is observed for **1a**

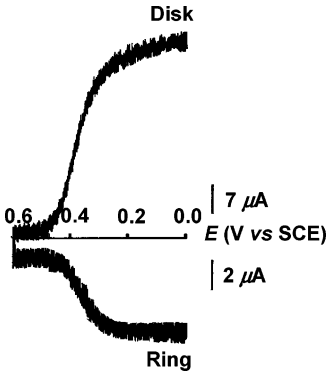

Figure 4. Reduction of O_2 at a rotating ring (Pt)−disk (EPG) electrode coated with **2** in air-saturated 1 M $HClO_4$. Collection efficiency N = 0.24. The potential of the ring electrode was maintained at 1.1 V. Rotation rate: 100 rpm. Scan rate: 5 mV s^{-1}.

except that more H_2O_2 is produced at the $E_{1/2}$ of 0.39 V (30%) than in the case of the porphyrin−corrole mixed oxidation state derivative where only 5% of H_2O_2 was observed. The biscorrole **3a** is thus less selective than the porphyrin−corrole dyad **1a** but more selective than the monocorrole **2** (55% H_2O_2). In comparison with the dicobalt porphyrin−corrole **1a** and biscorrole **3a**, the half-wave potential $E_{1/2}$ of the dioxygen reduction wave is less positive for the monomeric cobalt complex **2** (Table 1). Also, in the case of **2**, H_2O_2 is detected at the ring electrode as soon as dioxygen reduction occurs (Figure 4). Under these conditions, the value of n calculated from the disk and the ring currents is 2.9 at 0.38 V (Table 1). As complex **2** is not catalytically active toward the reduction of H_2O_2 (vide infra), this value of n requires that a portion of the dioxygen that reaches the electrode surface be reduced by four electrons to H_2O. The catalytic behavior of **2** is thus similar to what has been reported for cobalt porphyrins with unsubstituted meso positions such as (OEP)Co[32] or Co(II) porphine.[35] In both cases, a formation of dimers on the surface of the graphite electrode was proposed to explain the catalytic electroreduction of O_2 to H_2O.

Kinetics of O_2 Reduction Catalyzed by $(Me_4Ph_5Cor)Co$, 2, and $(PCA)Co_2$, 1a. Figure 5A shows a set of current−potential curves for the reduction of dioxygen at a rotating disk electrode coated with the cobalt monocorrole **2** and porphyrin−corrole **1a** in 1 M $HClO_4$. The corresponding Levich plot of limiting current vs the square root of the rotation rate $(\omega)^{1/2}$ and the lines calculated from the Levich equation for the diffusion-convection-limited two- and four-electron reduction of dioxygen are shown in Figure 5B. The Levich plot for monocorrole **2** shows that the steady-state limiting currents exceed the calculated values corresponding to the two-electron reduction of O_2. The nonlinearity of the Levich plot in Figure 5B suggests that the catalytic reaction is limited by a rate-determining step that precedes the electronic transfer (CE mechanism). This nonlinearity was previously observed for several cobalt(II) porphyrin complexes,[22,32,36−41] and the

(32) Song, E.; Shi, C.; Anson, F. C. *Langmuir* **1998**, *14*, 4315−4321.
(33) Erben, C.; Will, S.; Kadish, K. M. In *The Porphyrin Handbook*; Kadish, K. M., Smith, J. R. L., Guilard, R., Eds.; Academic Press: Boston, 2000; Vol. 2, pp 233−300.
(34) Licoccia, S.; Paolesse, R. *Struct. Bonding* **1995**, *84*, 71−133.
(35) Shi, C.; Steiger, B.; Yuasa, M.; Anson, F. C. *Inorg. Chem.* **1997**, *36*, 4294−4295.
(36) Durand, R. R., Jr.; Anson, F. C. *J. Electroanal. Chem.* **1982**, *134*, 273−289.
(37) Anson, F. C.; Ni, C.-L.; Saveant, J.-M. *J. Am. Chem. Soc.* **1985**, *107*, 3442−3450.
(38) Yuasa, M.; Steiger, B.; Anson, F. C. *J. Porphyrins Phthalocyanines* **1997**, *1*, 181−188.
(39) D'Souza, F.; Hsieh, Y.-Y.; Deviprasad, G. R. *Chem. Commun.* **1998**, 1027−1028.

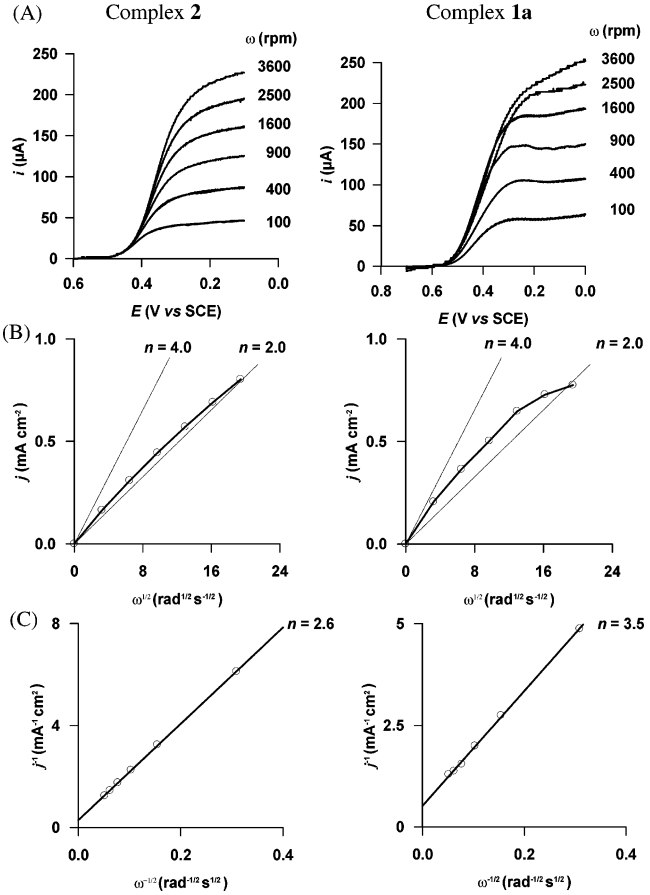

Figure 5. (A) Current−potential curves for the reduction of O_2 in 1 M $HClO_4$ at a rotating graphite disk electrode coated with 2.0×10^{-10} mol cm^{-2} of **2** (left) and 11.0×10^{-10} mol cm^{-2} of **1a** (right). Values of the rotational velocity (ω) of the electrode in rpm are indicated on each curve. The disk potential was scanned at 5 mV s^{-1}. (B) Levich plots of the rotating limiting currents (j) of (A) (○) vs square root of rotational velocity $(\omega)^{1/2}$. The lines refer to the theoretical curves for the $2e^-$ and $4e^-$ processes, as indicated in the figures. (C) Koutecký−Levich plots corresponding to B.

chemical step was assigned to the formation of a dioxygen adduct[42] which is a reducible species. Kinetic analysis of such systems is facilitated by means of Koutecký−Levich plots[43] of reciprocal current density $(j_{lim})^{-1}$ vs reciprocal square root of rotational velocity $(\omega)^{-1/2}$. Typical plots are shown in Figure 5C. These plots are interpreted on the basis of eq 1:

$$\frac{1}{j_{lim}} = \frac{1}{j_{lev}} + \frac{1}{j_k} \qquad (1)$$

where j_{lim} is the measured limiting current density (mA cm^{-2}). The Levich current, j_{lev}, and the kinetic current, j_k, that measure the rate of the current-limiting chemical reaction, are defined by eqs 2 and 3, respectively.

$$j_{lev} = 0.62nFD^{2/3}\upsilon^{-1/6}C^*\omega^{1/2} \qquad (2)$$

where n is the number of electrons transferred in the overall electrode reaction, F the Faraday constant (96485 C mol^{-1}), D and C^* are the diffusion coefficient (cm^2 s^{-1}) and bulk concentration of dioxygen (mol dm^{-3}), respectively, υ is the kinematic viscosity of water (cm^2 s^{-1}), and ω is the angular rotation speed (rad s^{-1}) of the electrode.

$$j_k = 10^3nFk\Gamma C^* \qquad (3)$$

where k (M^{-1} s^{-1}) is the second-order rate constant governing the current-limiting reaction between the reduced catalyst and O_2, and Γ (mol cm^{-2}) is the surface concentration of catalyst on the electrode that participates in catalyzing the reaction. The quantity of $(Me_4Ph_5Cor)Co$ present on the electrode ($\Gamma = 2.0 \times 10^{-10}$ mol cm^{-2}) was obtained by measuring the area under the cyclic voltammogram recorded in dioxygen-free 1 M $HClO_4$. The value of n determined from the slope of the Koutecký−Levich plot (Figure 5C) shows that a portion of dioxygen is reduced to water. This is in agreement with the value of $n = 2.9$ determined from the ring−disk experiment at a rotation speed of 100 rpm (Table 1). The value of the O_2 reduction rate constant k, evaluated at pH = 0, from the intercept of the Koutecký−Levich plot, is higher than previously reported rate constants governing the kinetics of the coordination of dioxygen to adsorbed cobalt(II) porphyrin complexes (Table 2).[42]

Table 2. Rate Constants (k) for the Electroreduction of O_2 by Adsorbed Catalysts in Air-Saturated Aqueous Acidic Solution (pH = 0)

catalyst	10^{-5} k, M^{-1} s^{-1}	ref[a]
$(PCA)Co_2$ (**1a**)	0.2	T.W.
$(Me_4Ph_5Cor)Co$ (**2**)	5.7	T.W.
$(FTF4)Co_2$	3.0	42
$(diethylesterMe_2Et_2P)Co$	1.4	42
$(DPA)Co_2$	0.2	30

[a] T.W. = This work.

The rotating disk procedure described above for measuring the rate constant governing the catalytic reaction of **2** with O_2 was also applied to the dicobalt porphyrin−corrole **1a**. An EPG disk was modified with $(PCA)Co_2$ using a dip-coating procedure (vide supra). The surface coverage of the disk was calculated from integration of the voltammetric peak recorded in a deoxygenated acidic solution (Figure 1A) and was found to be 11.0×10^{-10} mol cm^{-2} of geometric electrode area. The recorded hydrodynamic voltammograms in the presence of dioxygen are shown in Figure 5A. The Levich plot in Figure 5B is nonlinear, as expected for a reduction in which a current-limiting chemical step precedes the electron transfer. The reciprocal slope of the corresponding Koutecký−Levich plot (Figure 5C) corresponds to an apparent n value of 3.5 which suggests that O_2 is reduced to a mixture of H_2O and H_2O_2. This is also consistent with the magnitudes of the anodic ring currents at potentials on the plateau of the disk curent-potential curve in Figure 1B. The rate constant, k, for the catalytic reduction of O_2 by $(PCA)Co_2$ was evaluated from the intercept of the Koutecký−Levich plot (Figure 5C) and found to be 0.2×10^5 M^{-1} s^{-1} (Table 2). This value is lower than that obtained for the monocobalt porphyrin $(diethylesterMe_2Et_2P)Co$ ($k = 1.4 \times 10^5$ M^{-1} s^{-1})[42] and its related dimer $(FTF4)Co_2$ ($k = 3.0 \times 10^5$ M^{-1} s^{-1}),[42] but it is identical to that reported previously for the electrocatalytic reduction of O_2 in 1 M CF_3CO_2H by a $(DPA)Co_2$-coated graphite electrode where DPA = anthracenyl-bridged diporphyrin ($k = 0.2 \times 10^5$ M^{-1} s^{-1}).[30]

Thin-Layer Voltammetry. Further insight into the catalyzed reduction of dioxygen by **2** was obtained by dissolving the

(40) Steiger, B.; Anson, F. C. *Inorg. Chem.* **2000**, *39*, 4579−4585.
(41) Shi, C.; Anson, F. C. *Inorg. Chem.* **2001**, *40*, 5829−5833.
(42) Durand, R. R., Jr.; Bencosme, C. S.; Collman, J. P.; Anson, F. C. *J. Am. Chem. Soc.* **1983**, *105*, 2710−2718.
(43) Treimer, S.; Tang, A.; Johnson, D. C. *Electroanalysis* **2002**, *14*, 165−171.

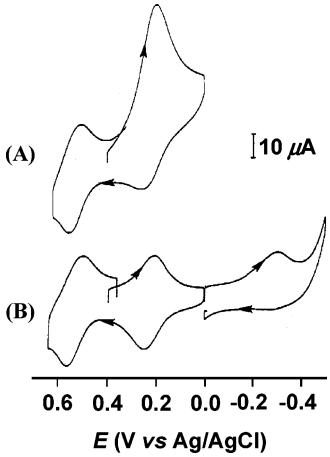

Figure 6. Cyclic voltammograms of **2** (0.6 mM) dissolved in a thin layer of acidified PhCN placed on an EPG electrode that was immersed in 1 M $HClO_4$. (A) In the presence of O_2 and (B) after the aqueous phase (and the equilibrated thin layer of PhCN) was saturated with argon. Scan rate: 50 mV s^{-1}.

catalyst in a thin layer of benzonitrile next to the electrode instead of adsorbing it directly on the electrode surface. Shown in Figure 6 are cyclic voltammograms obtained with an EPG electrode on which was placed a 30 μm layer of benzonitrile containing $(Me_4Ph_5Cor)Co$. The electrode was immersed in an aqueous solution of 1 M $HClO_4$. The large cathodic peak current at $E_p = 0.20$ V vs Ag/AgCl (Figure 6A) arises from the reduction of O_2 catalyzed by **2**. The rise in the catalytic current occurs at the same potential where, in the absence of O_2, $[(Me_4Ph_5Cor)Co^{IV}]^+$ is reduced to $[(Me_4Ph_5Cor)Co^{III}]^0$ in 1 M $HClO_4$ (Figure 6B). This implicates the cobalt(III) corrole as the catalytically active species. The reversible process observed at more cathodic potentials ($E_p = -0.30$ V vs Ag/AgCl) corresponds to the Co(III)/Co(II) redox couple.

Catalytic Activity of Cobalt Corrole Derivatives toward H_2O_2 at pH = 0. As shown by the rotating disk electrode voltammograms of $(Me_4Ph_5Cor)Co$ (Figure 5A), the reduction of O_2 proceeds in a single step, and H_2O_2 is the major product of the reduction at the plateau. In contrast, the larger disk current with $(PCA)Co_2$ (Figure 5A) shows that a portion of the O_2 is reduced to H_2O instead of H_2O_2. However, the catalyst may produce H_2O_2 as an intermediate species in the catalytic process. To test this possibility, the solution used to record the cyclic voltammogram in the presence of dioxygen (Figure 1) was made 0.5 mM in H_2O_2 and deoxygenated with argon for 20 min. The cyclic voltammogram recorded with a $(PCA)Co_2$-coated electrode in the presence of hydrogen peroxide is shown in Figure 7A. A catalytic oxidation peak of H_2O_2 to O_2 was observed at 0.65 V, whereas the reduction of the dioxygen formed at the electrode occurred at 0.42 V. No peak corresponding to the reduction of H_2O_2 to H_2O was detected between 0.80 and 0.00 V. The same electrochemical behavior was observed for $(Me_4Ph_5Cor)Co$ (Figure 7B) except that the magnitude of the oxidation peak current at 0.70 V was relatively higher than that of $(PCA)Co_2$. For a more quantitative assessment of the catalytic properties of complexes **1a** and **2** toward H_2O_2, current−potential curves were recorded at a rotating disk electrode in 1 M $HClO_4$ saturated with argon (Figure 8). Both adsorbed complexes catalyze the electrooxidation of H_2O_2 at $E_{1/2} = 0.61$ and 0.65 V, respectively. The decline in the limiting currents observed for **1a** and **2** at potentials higher than 0.80 V

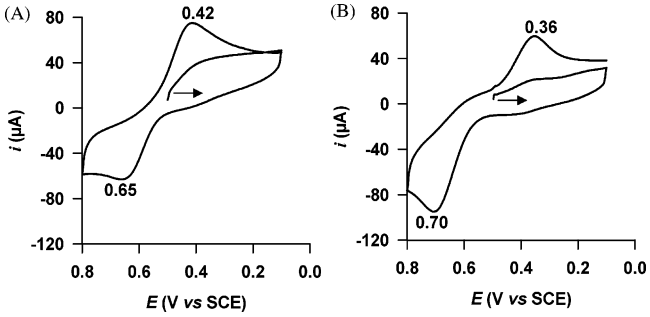

Figure 7. Cyclic voltammograms of **1a** (A) and **2** (B) adsorbed on EPG electrode. Supporting electrolyte: 1 M $HClO_4$ saturated with argon. $[H_2O_2] = 0.5$ mM. Scan rate: 50 mV s^{-1}.

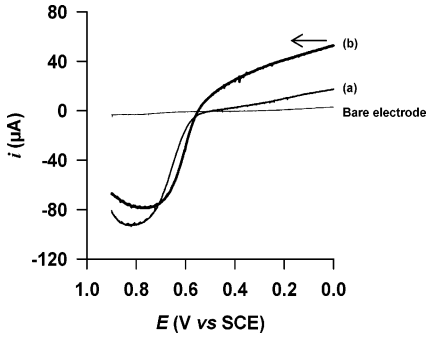

Figure 8. Rotating disk voltammograms of **2** (curve a) and **1a** (curve b) adsorbed on EPG electrode. Supporting electrolyte: 1 M $HClO_4$ saturated with argon. $[H_2O_2] = 0.5$ mM. Rotation rate: 100 rpm. Scan rate: 5 mV s^{-1}.

corresponds to a gradual loss of catalytic activity due to a possible degradation at the EPG surface. The curves for reduction of H_2O_2 examined at the $(Me_4Ph_5Cor)Co$-coated electrode reveal that cobalt(III) monocorrole **2** reduces H_2O_2 at a much lower rate than it catalyzes its oxidation. The RDE voltammogram recorded in a deoxygenated solution containing 0.5 mM H_2O_2 (curve a, Figure 8) shows a slow rise of the disk current from ca. 0.60 to 0.00 V. An analogous RDE experiment with a $(PCA)Co_2$-coated graphite disk (curve b, Figure 8) shows a relatively similar behavior of the dicobalt porphyrin−corrole dyad toward the catalytic reduction of H_2O_2. However, the magnitude of the cathodic currents recorded between 0.60 and 0.00 V are higher than that observed for the monocobalt corrole $(Me_4Ph_5Cor)Co$ (curve a, Figure 8). As expected, no oxidations or reductions of H_2O_2 were observed at the bare electrode, and this is also illustrated in Figure 8.

Collman et al. observed that a graphite electrode coated with $(FTF4)Co_2$ also catalyzes the two-electron reduction of H_2O_2 to H_2O in acidic media.[44] The catalytic reduction of H_2O_2 by $(FTF4)Co_2$ was characterized by rotating disk electrode voltammograms similar to those recorded for complex **1a** (Figure 8). A similar catalytic activity toward H_2O_2 was reported by Anson, Chang, and co-workers for a dicobalt cofacial diporphyrin, $(DPA)Co_2$, that is structurally similar to complex **1a**.[30] The lack of significant catalytic activity of $(DPA)Co_2$ toward the disproportionation of H_2O_2 was also demonstrated. Both Collman and Anson have stated that the rate of the electrocatalytic reduction of H_2O_2 by $(FTF4)Co_2$ and $(DPA)Co_2$ is very slow compared to the rate of O_2 reduction.[30,44] From

(44) Collman, J. P.; Hendricks, N. H.; Leidner, C. R.; Ngameni, E.; L'Her, M. *Inorg. Chem.* **1988**, *27*, 387−393.

the results shown in Figure 8 it is clear that this is also true for $(PCA)Co_2$.

Effect of Different Spacers on O_2 Catalysis. The dioxygen reduction catalytic properties of dicobalt porphyrin−corrole and biscorroles complexes bridged by biphenylene, 9,9-dimethylxanthene, dibenzofuran, and dibenzothiophene were compared to those of $(PCA)Co_2$ and $(BCA)Co_2$ (Chart 1). The electrochemical data are compiled in Table 1. The structural details on complexes with spacers of the type used in this study were reported previously.[18,45−47] The rigidity of the anthracene and biphenylene bridges in complexes **1a**, **1b**, **3a**, and **3b** minimize ring lateral slippage while maintaining a face-to-face arrangement of both macrocycles.[8] Biphenylene provides a tighter binding cavity than anthracene due to the fewer number of atoms separating the macrocyclic units. However, both single rigid linkers afford a small flexibility along the longitudinal axis of the ligands that allow the molecular clefts to structurally accommodate reaction intermediates during multielectron catalysis ("Pac-Man" effect[8,48]), resulting in an efficient catalytic reduction of O_2. The porphyrin−corrole dyads bridged by 9,9-dimethylxanthene (**1c**) and dibenzofuran (**1d**) also catalyze efficiently the direct four-electron reduction of O_2 to H_2O (Table 1) despite the structural difference between the two ligands. The xanthene bridge contains the same number of atoms as anthracene, whereas the five-membered ether ring in dibenzofuran increases the size of the binding pocket. The presence of an sp^3 oxygen in the latter bridge allows the molecular system to open and close its binding pocket by a longitudinal distance of over 4 Å in the presence of exogenous ligands as reported by Nocera et al.[48] This longitudinal flexibility is also observed in the case of complex **1d** since the PCO system displays four-electron reactivity toward dioxygen (Table 1).

Coatings of cobalt(III) biscorroles catalyze O_2 reduction at more negative potentials than do the $(PCY)Co_2$ systems (Table 1). The $E_{1/2}$ values of **3a**−**3c** are close to that observed for $(Me_4Ph_5Cor)Co$ ($E_{1/2}$ = 0.38 V), whereas complexes **3d** and **3e** reduce O_2 at more slightly negative potentials ($E_{1/2}$ = 0.35 V). Rotating ring−disk measurements show that the reduction of O_2 by $(BCY)Co_2$ complexes produces a more significant amount of H_2O_2 than that by porphyrin−corrole derivatives. In comparison with $(PCY)Co_2$ systems, the decrease of catalytic selectivity toward four-electron reduction of O_2 to H_2O in 1 M $HClO_4$ observed with $(BCY)Co_2$-coated electrodes suggests that the partially reduced dioxygen species is less stabilized. This decrease of selectivity for the direct reduction of O_2 to H_2O may be also explained by the difference of electronic properties between the electron-poor aryl-substituted corrole and the electron-rich alkyl-substituted porphyrin subunits. In comparison with **1**, the presence of a second cobalt(III) corrole unit in **3** may reduce the basicity of the oxygen adduct which strongly disfavors the four-electron pathway.[7]

Conclusions

In summary, we have shown that cobalt corroles can be used as effective catalysts in the reduction of O_2. The onset of dioxygen reduction occurs between 0.33 and 0.40 V for the 10 investigated catalysts when measured by cyclic voltammetry in 1 M $HClO_4$. However, the H_2O/H_2O_2 product ratios of the reduction differ in each case, with the most effective catalyst being the mixed oxidation state derivative **1a**−**1d** which leads almost exclusively to a four-electron reduction of O_2 at $E_{1/2}$ = 0.41−0.47 V vs SCE. A four-electron reduction also occurs to some extent in the absence of a porphyrin macrocycle; under these conditions O_2 reduction occurs at an $E_{1/2}$ of 0.35−0.39 V as seen in Table 1. Finally, reduction of hydrogen peroxide in 1 M $HClO_4$ by the dicobalt porphyrin−corrole **1a** is too slow to account for participation of free H_2O_2 as an intermediate in the four-electron reduction of O_2.

Acknowledgment. K.M.K. is grateful to the Robert A. Welch Foundation (Grant E-680) for support of this research as is L.K. for a predoctoral fellowship. The Région Bourgogne and CNRS are also acknowledged for financial support and for a BDI fellowship (F.B.).

JA0501060

(45) Kadish, K. M.; Burdet, F.; Jerome, F.; Barbe, J.-M.; Ou, Z.; Shao, J.; Guilard, R. *J. Organomet. Chem.* **2002**, *652*, 69.
(46) Barbe, J.-M.; Stern, C.; Pacholska, E.; Espinosa, E.; Guilard, R. *J. Porphyrins Phthalocyanines* **2004**, *8*, 301−312.
(47) Guilard, R.; Gros, C. P.; Barbe, J.-M.; Espinosa, E.; Jerome, F.; Tabard, A.; Latour, J.-M.; Shao, J.; Ou, Z.; Kadish, K. M. *Inorg. Chem.* **2004**, *43*, 7441−7455.
(48) Deng, Y.; Chang, C. J.; Nocera, D. G. *J. Am. Chem. Soc.* **2000**, *122*, 410−411.